Anaplastic Lymphoma Kinase Spares Organ Growth during Nutrient Restriction in *Drosophila*

Louise Y. Cheng,[1] Andrew P. Bailey,[1] Sally J. Leevers,[3] Timothy J. Ragan,[2] Paul C. Driscoll,[2] and Alex P. Gould[1,*]
[1]Division of Developmental Neurobiology
[2]Division of Molecular Structure
Medical Research Council National Institute for Medical Research, The Ridgeway, Mill Hill, London, NW7 1AA, UK
[3]Cancer Research UK London Research Institute, 44 Lincoln's Inn Fields, London, WC2A 3PX, UK
*Correspondence: agould@nimr.mrc.ac.uk

SUMMARY

Developing animals survive periods of starvation by protecting the growth of critical organs at the expense of other tissues. Here, we use *Drosophila* to explore the as yet unknown mechanisms regulating this privileged tissue growth. As in mammals, we observe in *Drosophila* that the CNS is more highly spared than other tissues during nutrient restriction (NR). We demonstrate that anaplastic lymphoma kinase (Alk) efficiently protects neural progenitor (neuroblast) growth against reductions in amino acids and insulin-like peptides during NR via two mechanisms. First, Alk suppresses the growth requirement for amino acid sensing via Slimfast/Rheb/TOR complex 1. And second, Alk, rather than insulin-like receptor, primarily activates PI3-kinase. Alk maintains PI3-kinase signaling during NR as its ligand, Jelly belly (Jeb), is constitutively expressed from a glial cell niche surrounding neuroblasts. Together, these findings identify a brain-sparing mechanism that shares some regulatory features with the starvation-resistant growth programs of mammalian tumors.

INTRODUCTION

The rate of growth (mass increase) during animal development is regulated in line with the availability of nutrients. Most animal species developing in the wild are subject to periods of nutrient deprivation and, to survive these, have evolved a range of protective mechanisms. Moderate nutrient deprivation often results in viable undersized adults, yet not all organs scale down isometrically with body size. For example, it has been known for many years that intrauterine growth restriction (IUGR) late in human gestation can result in small-for-gestational-age newborns with relatively large heads (Gruenwald, 1963). This asymmetric IUGR involves preferential growth of the central nervous system (CNS) at the expense of other organs, a process known as brain sparing (Dobbing and Sands, 1971). Although sparing of the brain and other vital organs is part of an important starvation survival strategy used by many developing animals, relatively little is known about the underlying molecular mechanisms.

Numerous studies of mouse knockouts and rare human mutations indicate that insulin/IGF ligands, together with their receptors and signal transduction pathways, are essential for fetal growth (reviewed by Engelman et al., 2006; Randhawa and Cohen, 2005). Insulin-like growth factor II (IGF-II) promotes fetal brain growth largely via its effects on placental size (Baker et al., 1993; Constância et al., 2002). In contrast, IGF-I synthesized by the brain itself appears to stimulate neural growth by local activation of the IGF type 1 receptor (IGF1R) in nestin-positive precursor cells (Beck et al., 1995; Liu et al., 1993; Liu et al., 2009; Sjögren et al., 1999; Yakar et al., 1999). Downstream of IGF1R, several conserved signal transduction components are required for brain growth, including insulin receptor substrate 2 (IRS2), class IA phosphatidylinositol 3-kinase (PI3K), Akt1 (PKBα), Akt3 (PKBγ) and the inhibitory phosphatase and tensin homolog (PTEN) (Bi et al., 1999; Chalhoub et al., 2009; Easton et al., 2005; Groszer et al., 2001; Schubert et al., 2003; Taguchi et al., 2007). In addition, the PI3K pathway intersects with a conserved amino acid-sensing pathway comprising target of rapamycin (Tor) kinase, Ras homolog enriched in brain (Rheb), and the negative regulators tuberous sclerosis complex 1 and 2 (TSC1/TSC2). Like the PI3K pathway, the TOR signaling pathway plays an essential role in fetal growth (reviewed by Polak and Hall, 2009; Zoncu et al., 2011). In mice, loss-of-function of Tor kinase inhibits cell proliferation in the developing brain, although some regions are more severely affected than others (Hentges et al., 1999).

The insect model organism, *Drosophila melanogaster,* develops via distinct embryonic, larval, pupal, and adult phases. The bulk of the larva, including the epidermis, muscles, gut, adipose tissue (fat body), and salivary glands, is composed of polyploid cells. The larva also contains smaller amounts of diploid tissues, such as the CNS and imaginal discs, which will function during adult life. Feeding larvae grow an impressive ~150-fold during 4 days, largely as a result of endoreplicating polyploid cells increasing in size. Diploid tissues also grow during the larval phase, but this occurs mostly by increasing cell number via mitotic divisions. A substantial body of evidence indicates that

the growth of diploid and polyploid tissues is strictly dependent upon the insulin-like peptides (Ilps)/ insulin-like receptor (InR)/ PI3K pathway and also upon the amino acid/TOR pathway (reviewed by Dann and Thomas, 2006; Edgar, 2006; Grewal, 2009; Shingleton et al., 2007; Teleman, 2010). Interestingly, however, partial inactivation of Tor or Rheb throughout the larva, or of Slimfast (Slif), an amino acid transporter lying upstream of Tor signaling within the fat body, reduces the growth of diploid imaginal discs less severely than that of polyploid salivary glands (Colombani et al., 2003; Oldham et al., 2000; Stocker et al., 2003; Zhang et al., 2000). It is also known that DNA replication is maintained more efficiently in the CNS and imaginal discs than in the gut or fat body when larvae are fed on a concentrated sucrose-only diet, lacking amino acids (Britton and Edgar, 1998). Together, these observations suggest that diploid tissues are less sensitive than polyploid tissues to growth inhibition by nutrient withdrawal, or by partial loss of insulin or TOR signaling.

In vivo genetic studies in mammals and many other species have, thus far, led to the notion that the growth of all developing animal tissues requires inputs from insulin/IGF receptors and from the amino acid-sensing TOR pathway. However, this hypothesis has not been thoroughly tested and, for some developing organs, the tissue-autonomous requirements for these signaling pathways are not yet known. Equally importantly, the molecular mechanisms permitting certain tissues to grow at the expense of others when nutrients are limiting remain largely unidentified. We now address both issues in *Drosophila* by quantifying, organ by organ, how growth and proliferation are affected by starvation and insulin/PI3K/TOR manipulations. Strikingly, at late-larval stages, we find that progenitors in the CNS are able to grow and divide at the normal rate during nutrient restriction that is severe enough to shut down all net body growth. Focus is then placed on identifying the key tissue-specific modifications in TOR and insulin/PI3K signaling that account for this brain-sparing mechanism.

RESULTS

Growth of the CNS Is Spared More Than that of Other Tissues

If *Drosophila* larvae are food deprived after attaining critical weight, at ~60 hr after larval hatching, they metamorphose into undersized adult flies with no developmental delay (Bakker, 1959; Beadle et al., 1938). In this study, we used a post-critical weight regime of severe but not total nutrient restriction (NR) from 60–96 hr (Figure 1A). This results in reduced hemolymph levels of Ilps (Géminard et al., 2009) (data not shown) and amino acids (Figure 1B). Under these NR conditions, we observed that the larval body attains less than half its normal fed size by pupariation at 96 hr (42% by mass, 45% by volume). However, the volumes of five different internal tissue/cell types do not all scale down isometrically with the body such that the CNS (mostly diploid) and the oenocytes (polyploid hepatocyte-like cells) (Gutierrez et al., 2007) display strong positive allometry at 96 hr (Figures 1C and 1D and Table S1 available online). For each organ, volume gains from 60–96 hr were then used to calculate the percentage of growth that is spared specifically during the fasting period (Figures 1C and 1E and Table S1; see the

Extended Experimental Procedures). From these measurements, it is clear that NR efficiently shuts down all net growth of the body and its internal polyploid tissues, such as the salivary gland, oenocytes, and adipose tissue (fat body). In contrast, the wing imaginal disc gains ~40% of its 8-fold volume increase and the CNS sustains ~50% of its 2-fold volume increase from 60–96 hr. These results demonstrate that the growth of diploid but not polyploid tissues is protected during NR and that not all diploid organs are equally spared.

To investigate the cellular basis for neural sparing, we focused on neuroblasts, the multipotent stem cell-like progenitors that generate most of the CNS. These undergo a series of asymmetric divisions, each time self-renewing and generating a ganglion mother cell (GMC) that, in turn, usually divides only once to produce two postmitotic neurons/glia (reviewed by Egger et al., 2008; Knoblich, 2010; Sousa-Nunes et al., 2010; Zhong and Chia, 2008). Using mosaic analysis (Lee and Luo, 1999), we GFP labeled single neuroblast lineages in the intact larva, calculating the overall volume of each clone (a measure of growth) and also the number of cells within each clone (a measure of proliferation). Remarkably, neuroblasts in NR larvae could still generate ~100% of their normal complement of neurons/glia by 96 hr (fed = 42 ± 3.2 cells, n = 15 clones; NR = 40 ± 1.4 cells, n = 10 clones). Likewise, the volumes of neuroblast clones do not differ significantly between fed and NR conditions (Figures 1C, 1E, and 2A). This striking finding contrasts with epithelial progenitors in the wing disc, where the NR regime spares only ~33% of clonal growth during 60–96 hr (Figures 1C, 1E, and 2B). Together, these results demonstrate that the generation of adult-specific neurons/glia by larval neuroblasts is highly prioritized, well above the 50% sparing of overall CNS growth, by a process that we refer to as super sparing.

CNS Growth Is Buffered against Changing Levels of Systemic Insulin-like Peptides

We next investigated whether a reduction in hemolymph Ilps would be sufficient to account for selective organ sparing during fasting. Ilps are secreted into the hemolymph from insulin-producing cells (IPCs) in the brain (Brogiolo et al., 2001; Ikeya et al., 2002; Rulifson et al., 2002). However, overexpressing *Ilp2* or an *Ilp2* RNA interference (RNAi) transgene (Broughton et al., 2008) within IPCs failed to alter body size significantly (Figure S1 and data not shown), suggesting compensation by posttranscriptional *Ilp2* regulation or by other Ilps (Broughton et al., 2008; Géminard et al., 2009; Grönke et al., 2010). We therefore developed an alternative method for manipulating Ilp levels. In mammals, PI3K signaling in pancreatic β cells acts at several levels to promote insulin secretion (Kaneko et al., 2010). Similarly, in *Drosophila*, we found that expressing activated PI3K within IPCs (*Ilp2 > p110^{CAAX}*) significantly increased IPC size, elevated Ilp2 hemolymph secretion by ~50% and boosted larval volume to 142% (Figure S1). *Ilp2* RNAi suppresses this body overgrowth, confirming that it is mediated via the observed increase in secreted Ilp2 (Figure S1). The converse IPC manipulation, expressing a PI3K inhibitor (*Ilp2 > p60*), moderately reduced IPC size and diminished larval volume to 72% (Figure S1). The size of the CNS and wing disc were not significantly affected by either IPC manipulation, indicating that both tissues are strongly
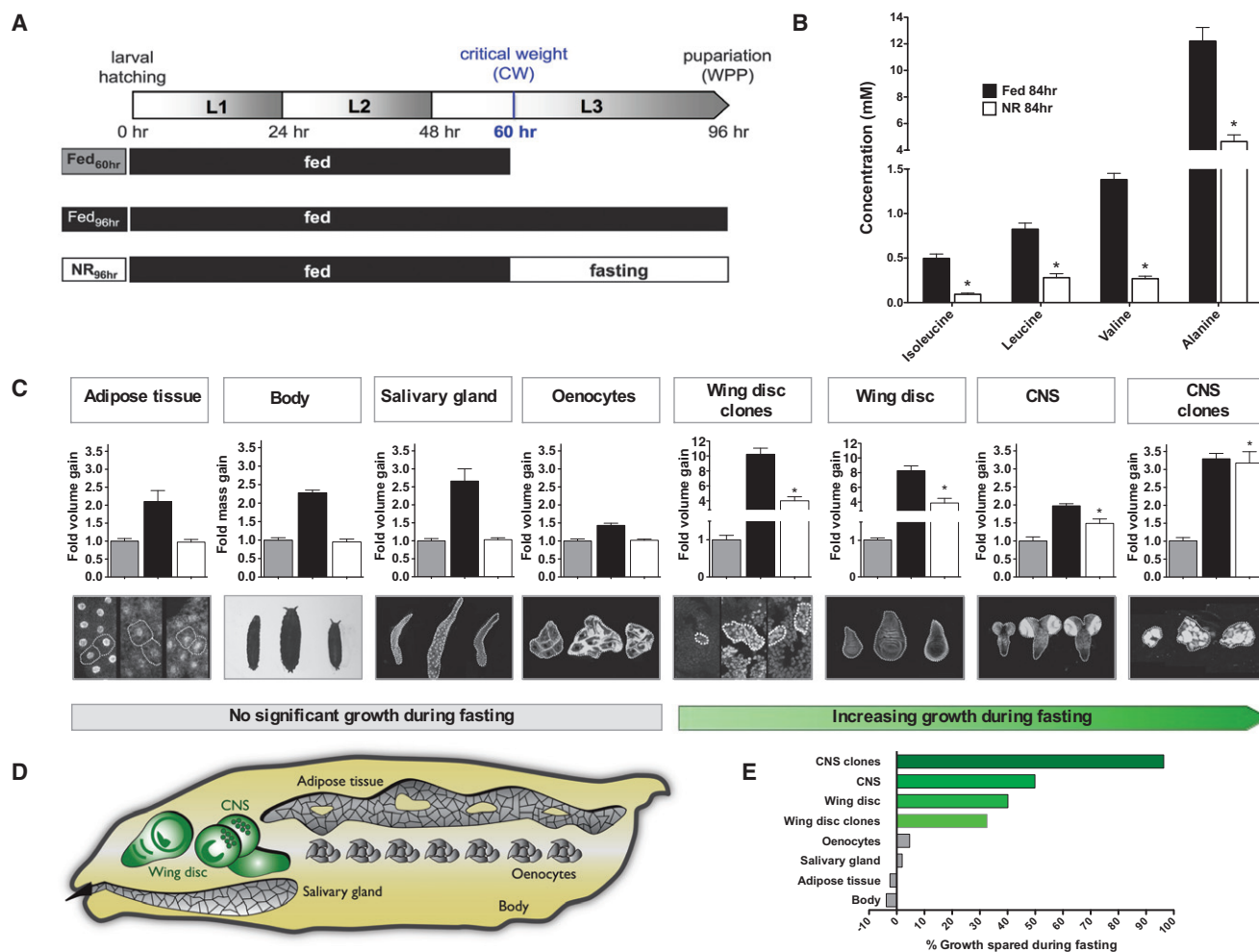
Figure 1. Organ Sparing during Fasting after Critical Weight

(A) Larval developmental timeline from 0–96 hr depicting the three larval instars (L1–L3) and, below, the three feeding/fasting regimes used in this study (Fed_{60hr}, Fed_{96hr}, and NR_{96hr}).

(B) Hemolymph concentrations of amino acids from fed and NR larvae at 84 hr.

(C) Histograms of fold volume gains, relative to Fed_{60hr}, for eight organs/clones/cells from Fed_{96hr} and NR_{96hr} larvae. All unprocessed volume measurements are given in Table S1. *$p < 0.001$ except for the CNS, where $p = 0.086$. In this, and all subsequent figures, error bars represent 1 standard error of the mean (SEM). Beneath each histogram are photomicrographs of Fed_{60hr} (left), Fed_{96hr} (middle), and NR_{96hr} (right) tissue.

(D) Schematic drawing of a larva depicting the tissue/cell types measured in (C). Most of the body, including the adipose tissue (fat body), salivary gland, and oenocytes are polyploid (gray). Imaginal tissues such as the wing disc and CNS are diploid (green). Note that each brain lobe of the CNS contains a cluster of seven insulin-producing cells (small green circles).

(E) Histograms of the percentage of growth spared during fasting between 60 and 96 hr. Polyploid tissues undergoing little/no net growth (gray) contrast with diploid tissues showing varying percentages of growth sparing (green).

See also Figure S1 and Table S1.

buffered, relative to the body, against changes in Ilps. Nevertheless, we previously showed that the CNS was spared to a higher degree than the wing disc during NR. Together, these findings suggest that the CNS is more strongly buffered than the wing disc against fluctuations in molecules other than Ilps, such as amino acids, which are also reduced during NR.

Slimfast, Rheb, and TORC1 Are Not Required for Larval Neuroblast Growth

To dissect the molecular basis for CNS super sparing, we analyzed components of the amino acid-sensing TOR pathway.

Larvae carrying a hypomorphic combination of *Tor* alleles that reduced body volume to 48% had a salivary gland of only 27% normal size, whereas the wing and CNS were 100% and 130% of wild-type volume respectively at 96 hr (Figure S2). This extends previous findings (Oldham et al., 2000) by showing that CNS growth is at least as resistant as imaginal disc growth to partial Tor inactivation. As the surprising CNS overgrowth in Tor hypomorphs could be due to influences from other tissues, we next used clonal analysis to measure cell-autonomous TOR pathway requirements. In wing discs, inactivation of *Slif*, *Rheb*, *Tor*, or the TOR complex 1 (TORC1) component *Raptor* severely
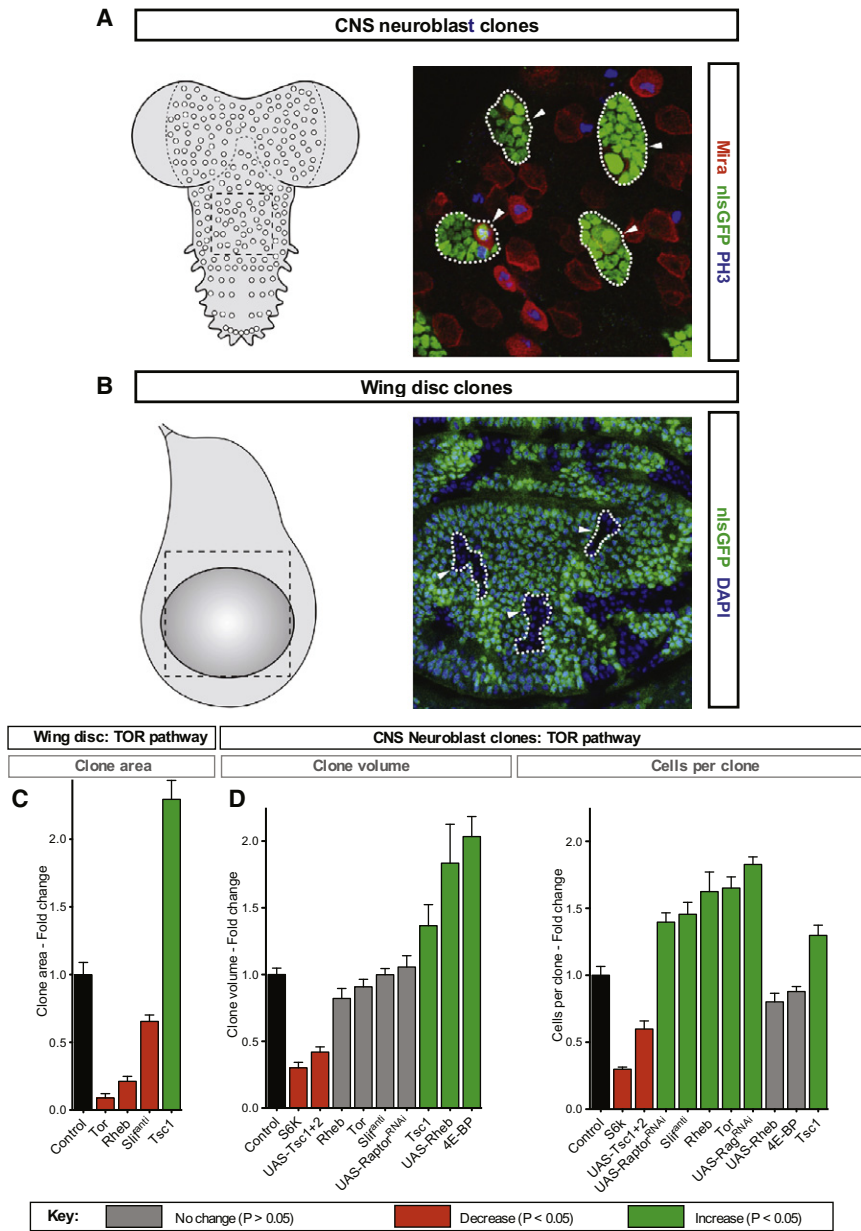
Figure 2. Functions of the TOR Pathway in Neuroblast and Wing Disc Clones

(A) Diagram of the larval CNS (left) indicating neuroblasts (small circles) indicate and the approximate thoracic field of view (dotted square) for the confocal image (right) showing four *tub > nlsGFP* marked neuroblast clones (dotted outlines) at 96 hr. Each clone contains one neuroblast (large Miranda-positive [Mira$^+$] cell) which, during M phase, expresses phosphorylated histone H3 (PH3).

(B) Diagram of a wing disc (left) indicating approximate field of view for the confocal image (right) showing multiple clones at 96 hr. Three *tub > nlsGFP* negative clones are indicated (dotted outlines).

(C and D) Histograms represent overexpression (*UAS*) or loss of function of the TOR pathway components indicated (see the main text for details and Table S2 for m, SEM, and n values for each genotype). Wing imaginal disc clones showing the relative clone area (mutant GFP$^-$/ wild-type twin-spot GFP$^+$ pixels) normalized to control clones (C). CNS neuroblast clones, showing the clone volume or the number of cells per clone, relative to controls (D). In this and all subsequent graphs, the key indicates that green bars represent an increase ($p < 0.05$), red bars a decrease ($p < 0.05$) and gray bars no significant change ($p > 0.05$) in t tests with the relevant paired controls.

See also Figure S2, Figure S3, and Figure S5.

clones (data not shown). However, hyperactivating the TOR pathway within neuroblast clones, by overexpressing *Rheb*, increases clonal growth without significantly affecting cell number (Figure 2D). Together with the loss-of-function results, we conclude that a large segment of the TOR pathway, from the Slif amino acid transporter downstream to TORC1, is not detectably required for the postembryonic growth of neuroblast clones but that its hyperactivation can nevertheless stimulate overgrowth.

In contrast to the unexpected lack of a growth input for Slif, Rheb, Tor, and Raptor, strong neural growth phenotypes are detected for two downstream TOR effectors: the translational activator S6-kinase (S6k) and the translational inhibitor 4E-BP/ Thor (Jünger et al., 2003; Montagne et al., 1999; Teleman et al., 2005). Loss of *S6k* activity reduced neuroblast clonal growth and cell number 4-fold, whereas loss of *4E-BP* activity doubled clonal growth without significantly affecting cell number (Figure 2D). The strong positive and negative growth inputs of S6k and 4E-BP, respectively, indicate that they are functional despite the lack of detectable growth inputs from their usual upstream regulators Slif, Rheb, Tor, and Raptor. Accordingly, *Tor* and/or *RagA* are required for Thr37/46 phosphorylation of

reduced clonal growth in a cell-autonomous manner, whereas loss of function of *Tsc1* greatly increased it (Figure 2C) (Colombani et al., 2003; Lee and Chung, 2007; Oldham et al., 2000; Stocker et al., 2003; Tapon et al., 2001; Zhang et al., 2000). In postembryonic neuroblast clones, loss-of-function for *Tsc1* similarly increased growth, yet, importantly, inactivation of *Slif*, *Rheb*, *TOR*, or *Raptor* had no significant growth effect in this tissue context (Figure 2D). Nevertheless, neuroblast clones lacking Slif, Rheb, Tor, or Raptor activity, as well as those expressing RNAi for RagA, a GTPase linking amino acid sensing to Tor activation (Kim et al., 2008), did contain ~50% more cells than normal (Figure 2D; see the Discussion). Consistent with this, cell proliferation is increased in *Tor* mutant neuroblast
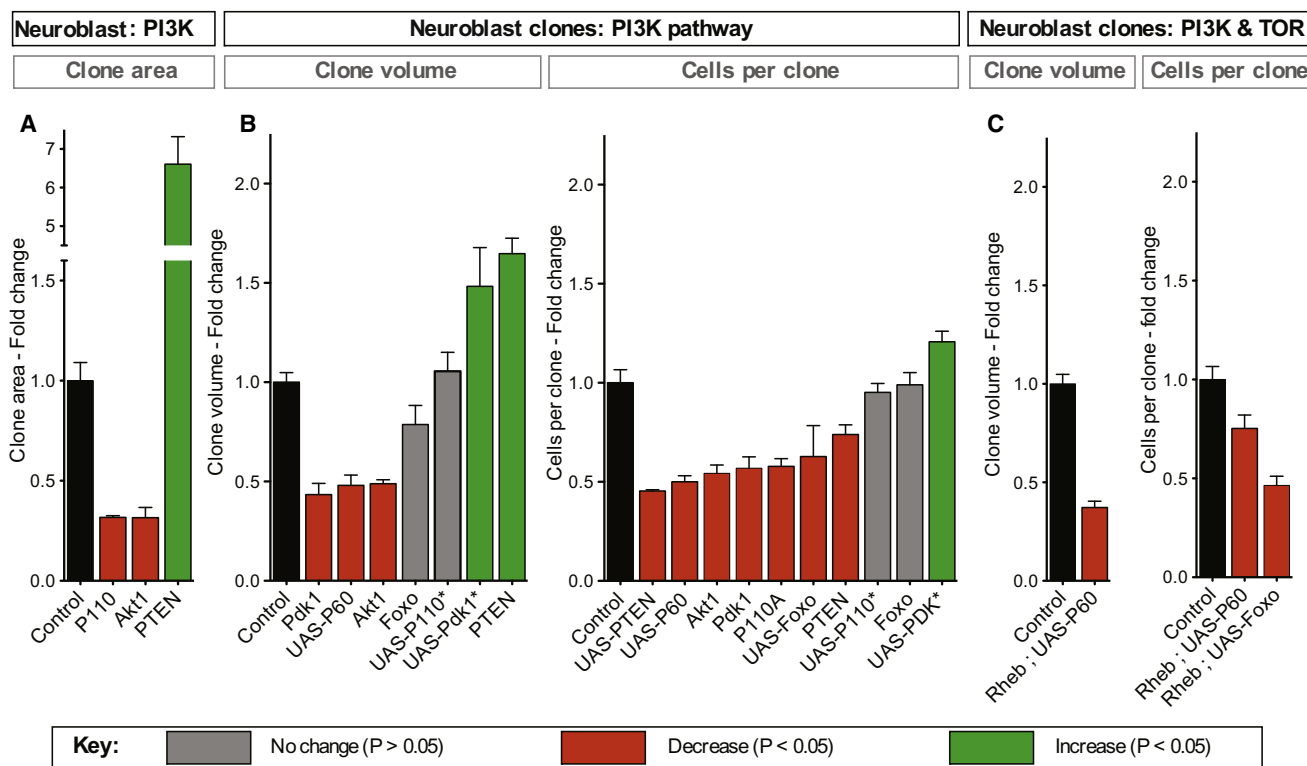
Figure 3. Functions of the PI3K Pathway in Neuroblast and Wing Disc Clones

Histograms represent overexpression (*UAS*) or loss of function of the PI3K and TOR pathway components indicated (see the main text for details and Table S2 for m, SEM, and n values for each genotype).

(A) Wing imaginal disc clones showing the relative area (mutant GFP⁻/wild-type GFP⁺ pixels), normalized to controls.

(B and C) CNS neuroblast clones showing the clone volume or the number of cells per clone, relative to controls.

See also Figure S4 and Figure S5.

4E-BP in fat body but not in neuroblasts (Figures S3A–S3C). Interestingly, Thr37/46 phosphorylation of 4E-BP predominates during M phase of the cell cycle in neuroblasts and in GMCs (Figure S3B). Consistent with *RagA/Tor* independence in both progenitor types, M phase phosphorylation of 4E-BP is retained during NR (Figure S3C). Hence, tissue-specific uncoupling of 4E-BP, and probably also S6k, from Slif amino acid sensing/TORC1 helps protect CNS growth from reduced dietary amino acids during NR.

The PI3K Signaling Pathway Is Required for Larval Neuroblast Growth

In the wing disc, PI3K signaling promotes growth such that loss-of-function clones for the gene encoding the catalytic subunit of class I PI3K (*p110*) or one of its downstream targets, *Akt1*, have a smaller-than-normal area (Figure 3A) (Verdu et al., 1999; Weinkove et al., 1999). Similarly, postembryonic neuroblast clones mutant for *Pdk1* or *Akt1* displayed an ~50% reduction in clonal volume and a corresponding decrease in cell number (Figure 3B). Comparable growth decreases were also measured in *p110* mutant clones and in clones overexpressing the PI3K signaling inhibitors *p60*, *Foxo*, or *PTEN* (Figure 4B). Conversely, PTEN inactivation increased neuroblast clonal growth by ~50% (Figure 3B). Surprisingly, however, these *PTEN* mutant clones

contained somewhat fewer cells than normal, correlating with a reduced cell-cycle speed and altered cyclin A/B expression but not with increased apoptosis (Figures S4E and S4F and data not shown). This unusual *PTEN* loss-of-function proliferation (but not growth) phenotype is suppressed by rapamycin, suggesting linkage with the atypical cell cycle-restraining role of TOR in neuroblast lineages (Figures 4A and 4B). We also found that overexpression an activated form of Pdk1 in neuroblast clones resulted in a modest increase in cell number and also in clonal volume (Figure 3B). In summary, growth in neuroblast lineages, as in other tissues, requires PI3K, Pdk1, and Akt1 and is inhibited by PTEN.

To characterize further the role of PI3K signaling, we analyzed *Akt1* mutant clones in detail and found that the neuroblast cell-cycle speed was reduced without disrupting asymmetric division or significantly increasing apoptosis (Figures S4A and S4B and data not shown). *Akt1* mutant neuroblasts finally cease dividing during pupal stages, after generating only about half the normal number of progeny (Figure S4C). We also used immunostaining for phosphorylated Akt (phospho-Akt) as a readout for PI3K signaling (Figure S5A) (Kockel et al., 2010). Due to background staining, we were unable to detect consistent decreases in phospho-Akt in clones lacking PI3K activity (Figure S5B). Despite this limitation, increases in
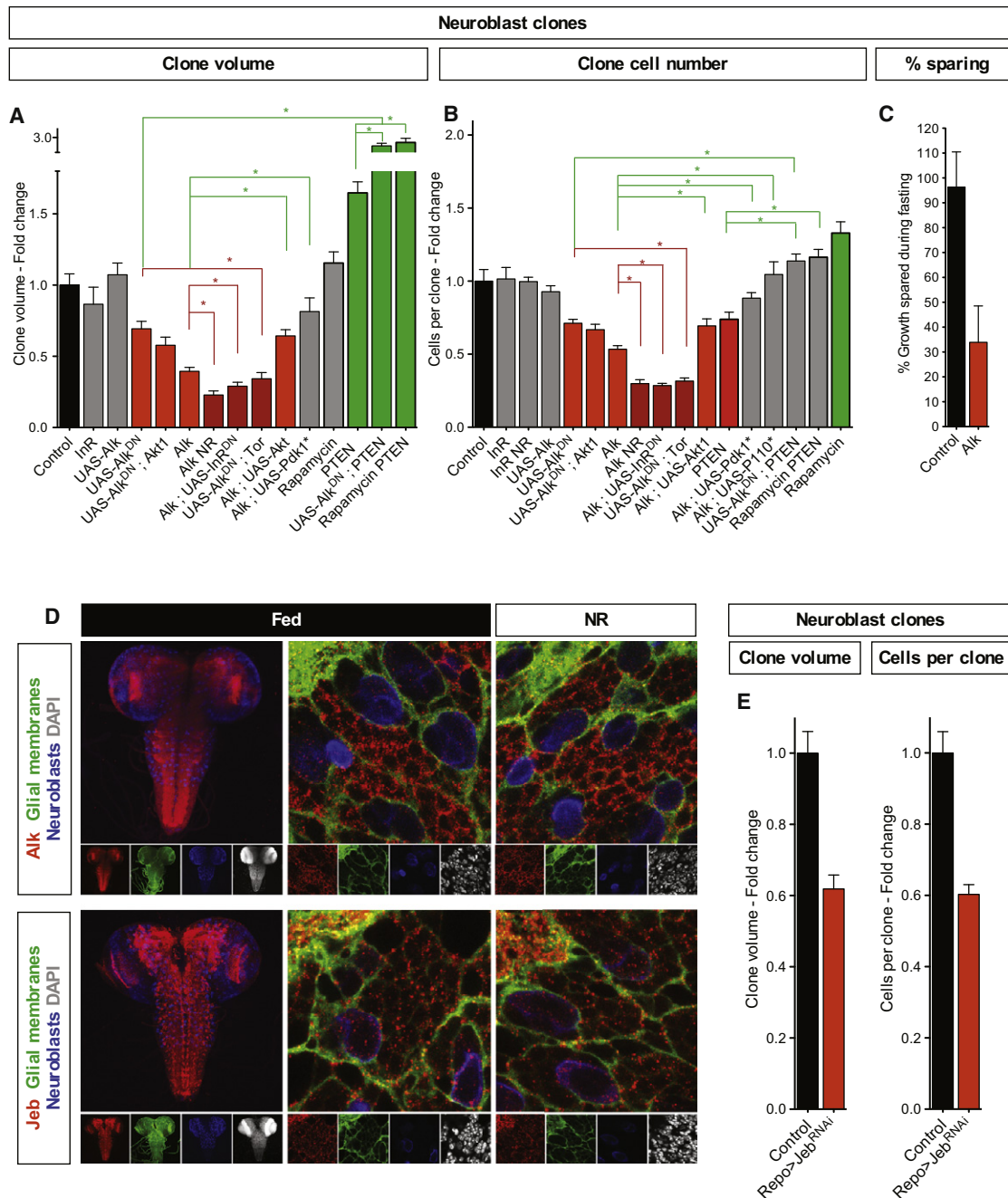
Figure 4. Jeb and Alk Regulate the Growth and Sparing of Neuroblast Clones

Histograms represent overexpression (*UAS*) or loss of function of the Alk, InR, PI3K and TOR pathway components indicated (see the main text for details and Table S2 for m, SEM, and n values for each genotype).

(A and B) CNS neuroblast clones showing clone volume (A) or number of cells per clone (B), relative to controls. Rapamycin, an inhibitor of TORC1 activity, is administered in the larval diet (Extended Experimental Procedures).

(C) Alk is required for CNS super sparing. Alk inactivation reduces the percentage of neuroblast clonal growth spared during the 60–96 hr fasting period from 96% to 34%.

(D) Alk and Jeb expression in the larval CNS. Alk protein is strongly expressed under fed and NR conditions in neurons and, at lower levels, in neuroblasts (large Mira$^+$ cells) and in glia (marked with *Repo > mGFP*). Jeb protein is strongly expressed under fed and NR conditions in glia but also localizes, at lower levels, in neuroblasts and in their neuronal progeny.

(E) Glial Jeb expression is required for the growth of neuroblast lineages. Neuroblast clones (marked with *nLacZ*) from heat-shocked *hsFlp; UAS-Jeb^{RNAi}; Repo-Gal4, act > > nLacZ* (*Repo > Jeb^{RNAi}*) larvae are significantly reduced in both volume and cell number, relative to those from controls.

See also Figure S4, Figure S5, and Figure S6.

phospho-Akt above background were reproducibly observed in clones expressing activated p110 and, more markedly, in strongly overgrowing clones lacking PTEN activity (Figure S5B). In contrast, neuroblast clones mutant for $Akt1^1$, encoding a phosphorylatable but kinase-inactive protein that can be used as a sensor for negative feedback in wing discs (Kockel et al., 2010), did not display elevated phospho-Akt (Figure S5B). Hence, S6k and TORC1-mediated negative feedbacks are unlikely to regulate Akt1 in neuroblast lineages. Together, the genetic and expression analyses demonstrate that PI3K signaling, kept in check by PTEN, is essential for the growth of neuroblast clones.

We then defined the regulatory relationship between PI3K and TOR signaling in neuroblast clonal growth and proliferation. As shown above, *Rheb* mutant neuroblast clones are normal in volume but contain excess cells, whereas *p60-* or *FoxO*-overexpressing clones are reduced in both volume and cell number. Combination of these TOR and PI3K pathway genotypes (*Rheb; UAS-p60* or *Rheb; UAS-FoxO*) resulted in neuroblast clones with reduced cell number and growth, demonstrating that *p60* or *FoxO* overexpression is epistatic to loss of *Rheb* activity (Figure 3C). This indicates that PI3K activity lies either downstream of *Rheb* repression or in a parallel pathway. To distinguish between these possibilities, we examined phospho-Akt levels in *Rheb* mutant neuroblast clones, but we did not observe any detectable increase (Figure S5B). These results show that, although Rheb is not detectably required for neuroblast clonal growth, it probably acts in parallel with PI3K to regulate proliferation.

Alk, Not InR, Activates PI3K Signaling and Growth in the Late-Larval CNS

We have shown that CNS growth requires PI3K signaling but is well buffered against reduced hemolymph Ilps. To investigate the molecular basis for Ilp-insensitive activation of PI3K, we first tested the role of the InR. At late-larval stages, InR activity is not required for neuroblast clonal growth or proliferation, irrespective of whether this is under fed or NR conditions (Figures 4A and 4B). We therefore sought to identify an alternative receptor tyrosine kinase (RTK) that might substitute for InR. By testing a panel of RTKs, we were able to find a strong growth requirement for *Drosophila* anaplastic lymphoma kinase (Alk) (Bazigou et al., 2007; Englund et al., 2003; Lee et al., 2003; Lorén et al., 2001, 2003). Alk is strongly expressed in the developing CNS (Lorén et al., 2001), and its catalytic domain has a higher sequence similarity to InR (4.5×10^{-61} E value) than to any other *Drosophila* RTK. Neuroblast lineages lacking Alk activity or expressing a dominant-negative form of Alk were strongly compromised by the late-larval stage, both in terms of their volume and cell number (Figures 4A and 4B). As with *Akt1* loss of function, *Alk* mutant clones retained an asymmetrically dividing neuroblast but failed to produce the full complement of neurons/glia by pupal stages (Figures S4B and S4C). Again similar to *Akt1*, this was associated with a slower cell cycle without any significant increase in cell death (Figures S4A and S4D). Thus, Alk, not InR, is required for the growth and proliferation of postembryonic neuroblast lineages.

To identify the Alk signal transduction pathway in neuroblasts, we first tested the role of the Ras/mitogen-activated protein kinase cascade, known to lie downstream of Alk in *Drosophila* (Englund et al., 2003; Lee et al., 2003). Surprisingly, neither loss of function of Ras1 nor overexpression of the activated form, Ras1^{V12}, significantly altered the number of cells in neuroblast clones (Figure S6). However, *Alk*-overexpressing neuroblasts did moderately upregulate phospho-Akt to levels comparable to those seen with activated p110, indicating that Alk activates the PI3K pathway (Figure S5B). Consistent with this, the *Alk* growth and proliferation phenotype was rescued by overexpressing activated p110 or Pdk1 and even wild-type Akt1 provided partial rescue (Figures 4A and 4B). Together, these results demonstrate that Alk promotes CNS growth by activating the PI3K pathway.

Alk Protects CNS Growth against Reduced *InR* and *Tor* Activity during NR

Importantly, NR halves both the volume and cell number of *Alk* mutant neuroblast clones at 96 hr (Figures 4A and 4B). Correspondingly, the percentage of neuroblast clonal growth spared during the fasting period falls markedly from 96% to 34% (Figure 4C). This demonstrates that Alk activity is essential for super sparing during fasting. Under fed conditions, comparable reductions in clonal volume and cell number at 96 hr were also observed in *Alk* mutant neuroblast clones simultaneously lacking *InR* (*Alk*; *UAS-InR^{DN}*) or *Tor* (*UAS-Alk^{DN}*; *Tor*) activities (Figures 4A and 4B). Hence, in the absence of *Alk* activity, *InR* and *Tor* in the CNS lose their atypical roles and revert to being positive growth and proliferation regulators, as they usually are in other tissues. *Alk* inhibition also significantly reduces the percentage of GMCs expressing Thr37/46 phosphorylated 4E-BP during M phase (Figure S3C). 4E-BP phosphorylation is further compromised in GMCs, and also in neuroblasts, by NR (*UAS-Alk^{DN}* NR) or by simultaneous removal of InR (*UAS-Alk^{DN}*; *UAS-InR^{DN}*) (Figure S3C). Together with the previous 4E-BP analysis, this indicates that Alk is required for NR-resistant 4E-BP phosphorylation in neural progenitors. In addition, the unusual requirement for *PTEN* as a positive cell-cycle (not growth) regulator in neuroblast clones reverts to the typical negative role when *Alk* activity is inhibited (*UAS-Alk^{DN}*; *PTEN*) (Figure 4B). Thus, *Alk* is required for the atypical CNS-specific regulation/function of at least four TOR/PI3K components: InR, Tor, 4E-BP, and PTEN. We conclude that *Alk* promotes CNS super sparing by suppressing the growth requirements for *Tor* and *InR*, thus enabling neuroblast lineages to be less reliant on amino acids and Ilps than other tissues.

The Alk Ligand, Jelly Belly, Is Expressed in Glia and Promotes CNS Growth

To determine the mechanism by which Alk is able to retain activity during NR, we first examined its expression pattern within the CNS. Under both fed and NR conditions, Alk protein was expressed at high levels in neurons and at lower levels in neuroblasts and glia (Figure 4D). The only known ligand for *Drosophila* Alk is Jelly belly (Jeb), a secreted LDL repeat containing protein that stimulates Alk signaling during visceral muscle development and photoreceptor axon guidance (Bazigou et al., 2007; Englund et al., 2003; Lee et al., 2003; Weiss et al., 2001). We found that the highest levels of Jeb protein are present in
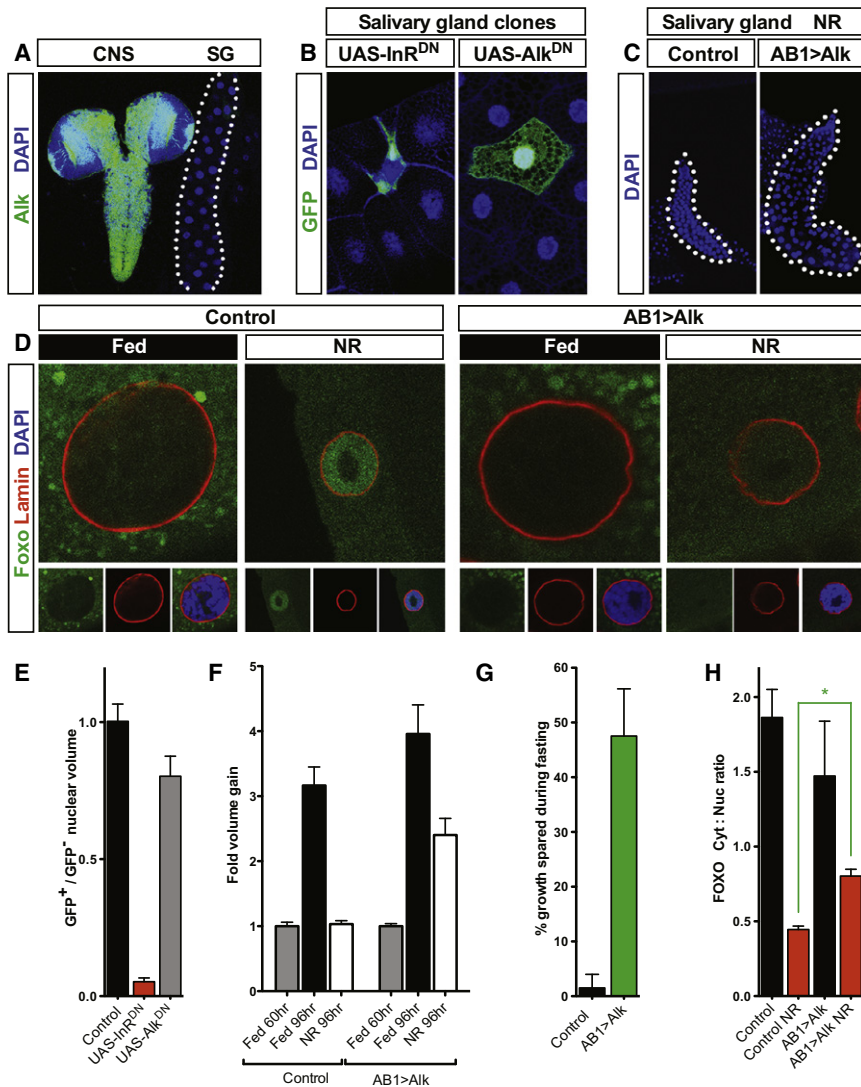
Figure 5. Ectopic Alk Expression in the Salivary Gland Induces Organ Sparing

(A) Alk is expressed strongly in the CNS but not in the salivary gland.

(B and E) Under fed conditions, salivary gland cells expressing $UAS\text{-}InR^{DN}$ (GFP$^+$) have a greatly reduced nuclear volume relative to their control (GFP$^-$) neighbors, whereas those expressing $UAS\text{-}Alk^{DN}$ (GFP$^+$) are not significantly different. Flp-out clones are GFP marked and DAPI stained in (B).

(C, F, and G) After NR, salivary gland volume at 96 hr (C, dotted outline) and percentage tissue growth spared during 60–96 hr fasting (F and G) both increase, relative to controls, when $UAS\text{-}Alk$ is expressed under the control of $AB1\text{-}GAL4$ ($AB1 > Alk$).

(D and H) Foxo cytoplasmic versus nuclear expression (D) and quantitation of the corresponding cytoplasmic/nuclear ratios (H) in salivary glands at 96 hr from control fed, control NR, $AB1 > Alk$ fed, and $AB1 > Alk$ NR larvae. Alk significantly reduces the accumulation of Foxo in salivary gland nuclei during fasting.

For histograms in (E)–(H), see Table S2 for m, SEM, and n values for each genotype.

See also Figure S3.

ysis revealed a strong growth requirement for InR but not for Alk (Figures 5A, 5B, and 5E). Wild-type $Drosophila$ Alk, when overexpressed, displays constitutive activity without Jeb (Lorén et al., 2001). We therefore ectopically expressed wild-type Alk in the salivary gland, either in clones or throughout the entire organ ($AB1 > Alk$), and we observed a large increase in the percentage of growth spared during the fasting period from ~2% to ~48% (Figures 5C, 5F, and 5G and data not shown). In line with this, Alk misexpression in salivary gland clones is also sufficient to stimulate Thr37/46 phosphorylation of 4E-BP under both fed and fasting conditions (Figure S3D). Finally, we used the cytoplasmic versus nuclear localization of the growth inhibitor Foxo as a readout for PI3K signaling (Delanoue et al., 2010; Puig et al., 2003). We found that Alk significantly reduces nuclear accumulation of Foxo during NR, almost doubling the cytoplasmic: nuclear ratio (Figures 5D and 5H). These results indicate that, in the salivary gland as in the CNS, Alk stimulates PI3K signaling and 4E-BP phosphorylation. Together, the salivary gland experiments also demonstrate that, unlike InR, Alk promotes tissue growth during NR, and it is sufficient to confer organ sparing on a nonspared tissue.

glia, with lower expression within the neuroblasts themselves and in their neuronal progeny (Figure 4D). Both Jeb and Alk are expressed strongly during fed and fasting conditions, indicating that Jeb/Alk signaling could function in CNS sparing (Figure 4D). Importantly, specific knockdown of Jeb in glia ($hsFlp$; $UAS\text{-}Jeb^{RNAi}$; $Repo\text{-}Gal4$, $actin > stop > nlacZ$) resulted in a significant ~40% reduction in both the volume and cell number of neuroblast clones (Figure 4E). Together, the expression and functional analyses demonstrate that glial synthesis of the Alk ligand Jeb is NR-resistant and is required in a non-cell-autonomous manner for the growth of neuroblast lineages.

Alk Misexpression in a Polyploid Tissue Confers Organ Sparing

We next addressed whether experimentally inducing Alk signaling in a nonspared polyploid tissue would be sufficient to protect its growth during fasting. The salivary gland expresses little or no detectable Alk and, consistent with this, clonal anal-

DISCUSSION

This study found that CNS progenitors are able to continue growing at their normal rate under fasting conditions severe

enough to shut down all net body growth. Jeb/Alk signaling was identified as a central regulator of this brain sparing, promoting tissue-specific modifications in TOR/PI3K signaling that protect growth against reduced amino acid and Ilp concentrations. These findings highlight that a "one size fits all" wiring diagram of the TOR/PI3K network should not be extrapolated between different cell types without experimental evidence. We now discuss the two molecular mechanisms by which Jeb/Alk signaling confers brain sparing and how they may be integrated into an overall model for starvation-resistant CNS growth.

Jeb/Alk Uncouples Slif Amino Acid Sensing from S6K and 4E-BP Growth Outputs

One mechanism by which Alk spares the CNS is by suppressing the growth requirement for amino acid sensing via Slif, Rheb, and TORC1 components in neuroblast lineages. An important finding here is that in the presence of Alk signaling *Tor* has no detectable growth input (evidence from *Tor* clones), but in its absence (evidence from *UAS-Alk^{DN}*; *Tor* clones) *Tor* reverts to its typical role as a positive regulator of both growth and proliferation. The growth requirement for Slif/TORC1 is clearly much less in the CNS than in other tissues such as the wing disc but a low-level input cannot be ruled out due to possible perdurance inherent in any clonal analysis. Although *Slif*, *Rheb*, *Tor*, and *Raptor* mutant neuroblast clones attain normal volume, this reflects increased cell numbers offset by reduced average cell size. Atypical suppression of proliferation by TORC1 has also been observed in wing discs, where partial inhibition with rapamycin advances G2/M progression (Wu et al., 2007).

Alk signaling in neuroblast lineages does not override the growth requirements for all TOR pathway components. The downstream effectors S6k and 4E-BP retain functions as positive and negative growth regulators, respectively. 4E-BP appears to be particularly critical in the CNS as mutant animals have normal mass (Teleman et al., 2005), but mutant neuroblast clones are twice their normal volume. In many tissues, 4E-BP is phosphorylated by nutrient-dependent TORC1 activity. In CNS progenitors, however, 4E-BP phosphorylation is regulated in an NR-resistant manner by Alk, not by TORC1. Hence, although the pathway linking Alk to 4E-BP is not yet clear, it makes an important contribution toward protecting CNS growth during fasting.

Jeb/Alk Substitutes for Ilps/InR during PI3K Signaling and Growth

A second mechanism by which Alk spares CNS growth is by maintaining PI3K signaling during NR. Alk suppresses or overrides the genetic requirement for InR in PI3K signaling, which may or may not involve the direct binding of intracellular domains as reported for human ALK and IGF-IR (Shi et al., 2009). Either way, in the CNS, glial Jeb expression stimulates Alk-dependent PI3K signaling and thus neural growth at similar levels during feeding and NR. In contrast, in tissues such as the salivary gland, where PI3K signaling is primarily dependent upon InR, falling Ilp concentrations during NR strongly reduce growth.

The finding that Alk signals via PI3K during CNS growth differs from the Ras/MAPK transduction pathway described in *Drosophila* visceral muscle (Englund et al., 2003; Lee et al.,

2003). However, a link between ALK and PI3K/Akt/Foxo signaling during growth is well documented in humans, both in glioblastomas and in non-Hodgkin lymphoma (Bai et al., 2000; Gu et al., 2004; Morris et al., 1994; Powers et al., 2002; Slupianek et al., 2001). Similarities with mammals are less obvious with regard to Alk ligands, as there is no clear Jeb ortholog and human ALK can be activated, directly or indirectly, by the secreted factors Pleiotrophin and Midkine (Bowden et al., 2002; Perez-Pinera et al., 2007; Stoica et al., 2002).

A Central Role for Jeb and Alk in CNS Super Sparing

A comparison of our results with those of previous studies indicates that CNS super sparing only becomes fully active at late-larval stages. Earlier in larval life, dietary amino acids are essential for neuroblasts to re-enter the cell cycle after a period of quiescence (Britton and Edgar, 1998). This nutrient-dependent reactivation involves a relay whereby Slif-dependent amino acid sensing in the fat body stimulates Ilp production from a glial cell niche (Sousa-Nunes et al., 2011). In turn, glial-derived Ilps activate InR and PI3K/TOR signaling in neuroblasts thus stimulating cell cycle re-entry (Chell and Brand, 2010; Sousa-Nunes et al., 2011). Hence, the relative importance of Ilps versus Jeb from the glial cell niche may change in line with the developmental transition of neuroblast growth from high to low nutrient sensitivity.

The results of this study suggest a working model for super sparing in the late-larval CNS (Figure 6; see the legend for details). Central to the model is that Jeb/Alk signaling suppresses Slif/RagA/Rheb/TORC1, InR, and 4E-BP functions and maintains S6k and PI3K activation, thus freeing CNS growth from the high dependence upon amino acid sensing and Ilps that exists in other organs. The CNS also contrasts with other spared diploid tissues such as the wing disc, in which PI3K-dependent growth requires a positive Tor input but is kept in check by negative feedback from TORC1 and S6K (Kockel et al., 2010; Zhang et al., 2000). Alk is both necessary (in the CNS) and sufficient (in the salivary gland) to promote organ growth during fasting. However, both Alk manipulations produce organ-sparing percentages intermediate between the 2% salivary gland and the 96% neuroblast values, arguing that other processes may also contribute. For example, some *Drosophila* tissues synthesize local sources of Ilps that could be more NR resistant than the systemic supply from the IPCs (Brogiolo et al., 2001; Okamoto et al., 2009; Slaidina et al., 2009). In mammals, this type of mechanism may contribute to brain sparing as it has been observed that IGF-I messenger RNA (mRNA) levels in the postnatal CNS are highly buffered against NR (Calikoglu et al., 2001). It will also be worthwhile exploring whether mammalian neural growth and brain sparing involve Alk and/or atypical TOR signaling. In this regard, it is intriguing that several studies show that activating mutations within the kinase domain of human ALK are associated with childhood neuroblastomas (Carén et al., 2008; Chen et al., 2008; George et al., 2008; Janoueix-Lerosey et al., 2008; Mossé et al., 2008). In addition, fetal growth of the mouse brain was recently reported to be resistant to loss of function of TORC1 (Zou et al., 2011). Finally, a comparison between our findings and those of a cancer study (Kalaany and Sabatini, 2009), highlights that insulin/IGF independence and constitutive
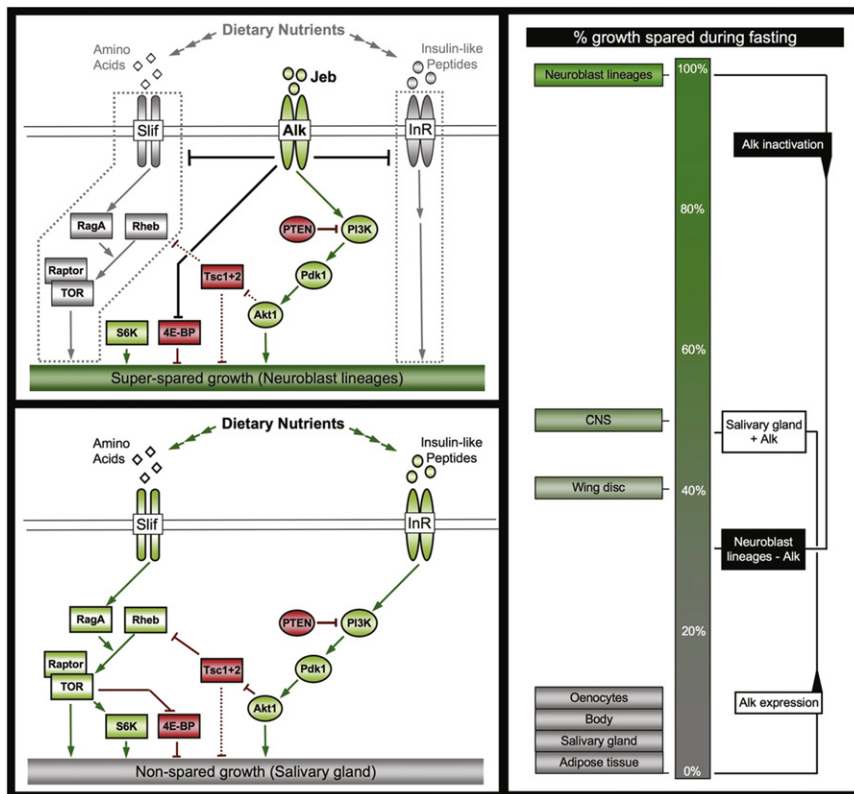
Figure 6. Alk Regulates CNS Sparing via the TOR and PI3K Pathways

The panels on the left show the genetic interactions between Alk, InR, TOR, and PI3K signaling components in the super-spared CNS (upper panel) and in the unspared salivary gland (lower panel). The genetic circuitry (direct or indirect interactions) depicted for super-spared growth in neuroblast lineages is a working model from this study, whereas the circuitry from nonspared growth in the salivary gland is derived from previous studies (see the main text for details). Growth-promoting (green), growth-inhibiting (red), and growth-neutral (gray) components are indicated. The vertical ruler (right panel) depicts percentage sparing of growth during late-larval fasting for individual organs. Alk inactivation in CNS neuroblast clones (Neuroblast lineages – Alk) dramatically reduces sparing, and, conversely, ectopic expression of Alk in the salivary gland (Salivary gland + Alk) strongly increases sparing.

PI3K activity are features of NR-resistant growth in contexts as diverse as insect CNS development and human tumorigenesis.

EXPERIMENTAL PROCEDURES

Drosophila Genetics, Clone Induction, Organ, Cell, Clone, and Hemolymph Measurements

Descriptions of most genetic elements can be found in Flybase (Drysdale et al., 2005) (http://flybase.bio.indiana.edu/). Developmental timings, relative to larval hatching at 0 hr, were calculated chronologically except for the 96 hr stage, which was selected by morphological and behavioral criteria. Unless stated otherwise, all larvae were dissected for tissue, clone or cell analysis at critical weight (60 hr) or at the wandering L3 stage (96 hr). CNS neuroblast clones were induced for 1 hr at 37°C at 24–30 hr. Twin spot clones in wing discs were induced for 45 min at 37°C at 24–36 hr. Salivary gland flipout clones were induced for 7 min at the end of embryogenesis. Details of genetic strains, antibodies, immunostaining, and further details of organ, cell, clone, and hemolymph measurements are provided in the Extended Experimental Procedures. In brief, body mass was measured in triplicate for groups of five white prepupae. Body volumes were estimated with the formula $\pi r^2 l$. Tissue and clone volume measurements were acquired from 3D reconstructions of 1.5 μm spaced confocal Z stacks with Volocity software (Improvision) or Amira 5 (Visage Imaging). Areas of GFP+ and GFP− twin spot clones in wing discs were calculated using Leica LAS software and the Image J (National Institutes of Health) plug-ins "freehand selection" and "measure." Volumes of salivary gland nuclei were estimated with the formula $4/3\pi r^3$, with r measured from single confocal sections using the Leica LAS software to average orthogonal measurements of nuclear diameter (2r). For each organ/clone/cell type, the percentage growth spared during the fasting period was calculated with the formula (Volume NR$_{96hr}$ – Volume Fed$_{60hr}$) ÷ (Volume Fed$_{96hr}$ – Volume Fed$_{60hr}$) × 100%. Flag-tagged Ilp2 was measured in hemolymph with western

blotting as described (Géminard et al., 2009). Amino acid concentrations were measured by nuclear magnetic resonance analysis of hemolymph derived from groups of 20 larvae under fed and NR conditions.

Larval Dietary Manipulations

Drosophila were raised at 25°C on our standard cornmeal/yeast/agar medium (composition in Gutierrez et al., 2007) supplemented with live bakers yeast granules, unless otherwise stated. For NR experiments, larvae were raised on our standard medium and selected morphologically 0–1 hr after the L2-to-L3 molt, then aged a further 12 hr to attain critical weight. Larvae were then transferred to NR medium (1% agarose/PBS) in 1.5 ml microcentrifuge tubes, plugged with nonabsorbant cotton wool, until 96 hr.

SUPPLEMENTAL INFORMATION

Supplemental Information includes Extended Experimental Procedures, six figures, and two tables and can be found with this article online at doi:10.1016/j.cell.2011.06.040.

REFERENCES

Bai, R.Y., Ouyang, T., Miething, C., Morris, S.W., Peschel, C., and Duyster, J. (2000). Nucleophosmin-anaplastic lymphoma kinase associated with anaplastic large-cell lymphoma activates the phosphatidylinositol 3-kinase/Akt antiapoptotic signaling pathway. Blood 96, 4319–4327.

Baker, J., Liu, J.P., Robertson, E.J., and Efstratiadis, A. (1993). Role of insulin-like growth factors in embryonic and postnatal growth. Cell 75, 73–82.

Bakker, K. (1959). Feeding period, growth and pupation in larvae of Drosophila melanogaster. Entomol. Exp. Appl. 2, 171–186.

Bazigou, E., Apitz, H., Johansson, J., Lorén, C.E., Hirst, E.M., Chen, P.L., Palmer, R.H., and Salecker, I. (2007). Anterograde Jelly belly and Alk receptor tyrosine kinase signaling mediates retinal axon targeting in Drosophila. Cell 128, 961–975.

Beadle, G.W., Tatum, E.L., and Clancy, C.W. (1938). Food level in relation to rate of development and eye pigmentation in Drosophila. Biol. Bull. 75, 447–462.

Beck, K.D., Powell-Braxton, L., Widmer, H.R., Valverde, J., and Hefti, F. (1995). Igf1 gene disruption results in reduced brain size, CNS hypomyelination, and loss of hippocampal granule and striatal parvalbumin-containing neurons. Neuron 14, 717–730.

Bi, L., Okabe, I., Bernard, D.J., Wynshaw-Boris, A., and Nussbaum, R.L. (1999). Proliferative defect and embryonic lethality in mice homozygous for a deletion in the p110alpha subunit of phosphoinositide 3-kinase. J. Biol. Chem. 274, 10963–10968.

Bowden, E.T., Stoica, G.E., and Wellstein, A. (2002). Anti-apoptotic signaling of pleiotrophin through its receptor, anaplastic lymphoma kinase. J. Biol. Chem. 277, 35862–35868.

Britton, J.S., and Edgar, B.A. (1998). Environmental control of the cell cycle in Drosophila: nutrition activates mitotic and endoreplicative cells by distinct mechanisms. Development 125, 2149–2158.

Brogiolo, W., Stocker, H., Ikeya, T., Rintelen, F., Fernandez, R., and Hafen, E. (2001). An evolutionarily conserved function of the Drosophila insulin receptor and insulin-like peptides in growth control. Curr. Biol. 11, 213–221.

Broughton, S., Alic, N., Slack, C., Bass, T., Ikeya, T., Vinti, G., Tommasi, A.M., Driege, Y., Hafen, E., and Partridge, L. (2008). Reduction of DILP2 in Drosophila triages a metabolic phenotype from lifespan revealing redundancy and compensation among DILPs. PLoS ONE 3, e3721.

Calikoglu, A., Karayal, A., and D'Ercole, A. (2001). Nutritional regulation of IGF-I expression during brain development in mice. Pediatr. Res. 49, 197–202.

Carén, H., Abel, F., Kogner, P., and Martinsson, T. (2008). High incidence of DNA mutations and gene amplifications of the ALK gene in advanced sporadic neuroblastoma tumours. Biochem. J. 416, 153–159.

Chalhoub, N., Zhu, G., Zhu, X., and Baker, S.J. (2009). Cell type specificity of PI3K signaling in Pdk1- and Pten-deficient brains. Genes Dev. 23, 1619–1624.

Chell, J.M., and Brand, A.H. (2010). Nutrition-responsive glia control exit of neural stem cells from quiescence. Cell 143, 1161–1173.

Chen, Y., Takita, J., Choi, Y.L., Kato, M., Ohira, M., Sanada, M., Wang, L., Soda, M., Kikuchi, A., Igarashi, T., et al. (2008). Oncogenic mutations of ALK kinase in neuroblastoma. Nature 455, 971–974.

Colombani, J., Raisin, S., Pantalacci, S., Radimerski, T., Montagne, J., and Léopold, P. (2003). A nutrient sensor mechanism controls Drosophila growth. Cell 114, 739–749.

Constância, M., Hemberger, M., Hughes, J., Dean, W., Ferguson-Smith, A., Fundele, R., Stewart, F., Kelsey, G., Fowden, A., Sibley, C., and Reik, W. (2002). Placental-specific IGF-II is a major modulator of placental and fetal growth. Nature 417, 945–948.

Dann, S.G., and Thomas, G. (2006). The amino acid sensitive TOR pathway from yeast to mammals. FEBS Lett. 580, 2821–2829.

Delanoue, R., Slaidina, M., and Léopold, P. (2010). The steroid hormone ecdysone controls systemic growth by repressing dMyc function in Drosophila fat cells. Dev. Cell 18, 1012–1021.

Dobbing, J., and Sands, J. (1971). Vulnerability of developing brain. IX. The effect of nutritional growth retardation on the timing of the brain growth-spurt. Biol. Neonate 19, 363–378.

Drysdale, R.A., and Crosby, M.A.; FlyBase Consortium. (2005). FlyBase: genes and gene models. Nucleic Acids Res. 33(Database issue), D390–D395.

Easton, R.M., Cho, H., Roovers, K., Shineman, D.W., Mizrahi, M., Forman, M.S., Lee, V.M., Szabolcs, M., de Jong, R., Oltersdorf, T., et al. (2005). Role for Akt3/protein kinase Bgamma in attainment of normal brain size. Mol. Cell. Biol. 25, 1869–1878.

Edgar, B.A. (2006). How flies get their size: genetics meets physiology. Nat. Rev. Genet. 7, 907–916.

Egger, B., Chell, J.M., and Brand, A.H. (2008). Insights into neural stem cell biology from flies. Philos. Trans. R. Soc. Lond. B Biol. Sci. 363, 39–56.

Engelman, J.A., Luo, J., and Cantley, L.C. (2006). The evolution of phosphatidylinositol 3-kinases as regulators of growth and metabolism. Nat. Rev. Genet. 7, 606–619.

Englund, C., Lorén, C.E., Grabbe, C., Varshney, G.K., Deleuil, F., Hallberg, B., and Palmer, R.H. (2003). Jeb signals through the Alk receptor tyrosine kinase to drive visceral muscle fusion. Nature 425, 512–516.

Géminard, C., Rulifson, E.J., and Léopold, P. (2009). Remote control of insulin secretion by fat cells in Drosophila. Cell Metab. 10, 199–207.

George, R.E., Sanda, T., Hanna, M., Fröhling, S., Luther, W., 2nd, Zhang, J., Ahn, Y., Zhou, W., London, W.B., McGrady, P., et al. (2008). Activating mutations in ALK provide a therapeutic target in neuroblastoma. Nature 455, 975–978.

Grewal, S.S. (2009). Insulin/TOR signaling in growth and homeostasis: a view from the fly world. Int. J. Biochem. Cell Biol. 41, 1006–1010.

Grönke, S., Clarke, D.F., Broughton, S., Andrews, T.D., and Partridge, L. (2010). Molecular evolution and functional characterization of Drosophila insulin-like peptides. PLoS Genet. 6, e1000857.

Groszer, M., Erickson, R., Scripture-Adams, D.D., Lesche, R., Trumpp, A., Zack, J.A., Kornblum, H.I., Liu, X., and Wu, H. (2001). Negative regulation of neural stem/progenitor cell proliferation by the Pten tumor suppressor gene in vivo. Science 294, 2186–2189.

Gruenwald, P. (1963). Chronic Fetal Distress and Placental Insufficiency. Biol. Neonat. 5, 215–265.

Gu, T.L., Tothova, Z., Scheijen, B., Griffin, J.D., Gilliland, D.G., and Sternberg, D.W. (2004). NPM-ALK fusion kinase of anaplastic large-cell lymphoma regulates survival and proliferative signaling through modulation of FOXO3a. Blood 103, 4622–4629.

Gutierrez, E., Wiggins, D., Fielding, B., and Gould, A.P. (2007). Specialized hepatocyte-like cells regulate Drosophila lipid metabolism. Nature 445, 275–280.

Hentges, K., Thompson, K., and Peterson, A. (1999). The flat-top gene is required for the expansion and regionalization of the telencephalic primordium. Development 126, 1601–1609.

Ikeya, T., Galic, M., Belawat, P., Nairz, K., and Hafen, E. (2002). Nutrient-dependent expression of insulin-like peptides from neuroendocrine cells in the CNS contributes to growth regulation in Drosophila. Curr. Biol. 12, 1293–1300.

Janoueix-Lerosey, I., Lequin, D., Brugières, L., Ribeiro, A., de Pontual, L., Combaret, V., Raynal, V., Puisieux, A., Schleiermacher, G., Pierron, G., et al. (2008). Somatic and germline activating mutations of the ALK kinase receptor in neuroblastoma. Nature 455, 967–970.

Jünger, M.A., Rintelen, F., Stocker, H., Wasserman, J.D., Végh, M., Radimerski, T., Greenberg, M.E., and Hafen, E. (2003). The Drosophila forkhead transcription factor FOXO mediates the reduction in cell number associated with reduced insulin signaling. J. Biol. 2, 20.

Kalaany, N.Y., and Sabatini, D.M. (2009). Tumours with PI3K activation are resistant to dietary restriction. Nature 458, 725–731.

Kaneko, K., Ueki, K., Takahashi, N., Hashimoto, S., Okamoto, M., Awazawa, M., Okazaki, Y., Ohsugi, M., Inabe, K., Umehara, T., et al. (2010). Class IA phosphatidylinositol 3-kinase in pancreatic β cells controls insulin secretion by multiple mechanisms. Cell Metab. 12, 619–632.

Kim, E., Goraksha-Hicks, P., Li, L., Neufeld, T.P., and Guan, K.L. (2008). Regulation of TORC1 by Rag GTPases in nutrient response. Nat. Cell Biol. 10, 935–945.

Knoblich, J.A. (2010). Asymmetric cell division: recent developments and their implications for tumour biology. Nat. Rev. Mol. Cell Biol. 11, 849–860.

Kockel, L., Kerr, K.S., Melnick, M., Brückner, K., Hebrok, M., and Perrimon, N. (2010). Dynamic switch of negative feedback regulation in Drosophila Akt-TOR signaling. PLoS Genet. 6, e1000990.

Lee, G., and Chung, J. (2007). Discrete functions of rictor and raptor in cell growth regulation in Drosophila. Biochem. Biophys. Res. Commun. 357, 1154–1159.

Lee, T., and Luo, L. (1999). Mosaic analysis with a repressible cell marker for studies of gene function in neuronal morphogenesis. Neuron 22, 451–461.

Lee, H.-H., Norris, A., Weiss, J.B., and Frasch, M. (2003). Jelly belly protein activates the receptor tyrosine kinase Alk to specify visceral muscle pioneers. Nature 425, 507–512.

Liu, J.P., Baker, J., Perkins, A.S., Robertson, E.J., and Efstratiadis, A. (1993). Mice carrying null mutations of the genes encoding insulin-like growth factor I (Igf-1) and type 1 IGF receptor (Igf1r). Cell 75, 59–72.

Liu, W., Ye, P., O'Kusky, J.R., and D'Ercole, A.J. (2009). Type 1 insulin-like growth factor receptor signaling is essential for the development of the hippocampal formation and dentate gyrus. J. Neurosci. Res. 87, 2821–2832.

Lorén, C.E., Scully, A., Grabbe, C., Edeen, P.T., Thomas, J., McKeown, M., Hunter, T., and Palmer, R.H. (2001). Identification and characterization of DAlk: a novel Drosophila melanogaster RTK which drives ERK activation in vivo. Genes Cells 6, 531–544.

Lorén, C.E., Englund, C., Grabbe, C., Hallberg, B., Hunter, T., and Palmer, R.H. (2003). A crucial role for the Anaplastic lymphoma kinase receptor tyrosine kinase in gut development in Drosophila melanogaster. EMBO Rep. 4, 781–786.

Montagne, J., Stewart, M.J., Stocker, H., Hafen, E., Kozma, S.C., and Thomas, G. (1999). Drosophila S6 kinase: a regulator of cell size. Science 285, 2126–2129.

Morris, S.W., Kirstein, M.N., Valentine, M.B., Dittmer, K.G., Shapiro, D.N., Saltman, D.L., and Look, A.T. (1994). Fusion of a kinase gene, ALK, to a nucleolar protein gene, NPM, in non-Hodgkin's lymphoma. Science 263, 1281–1284.

Mossé, Y.P., Laudenslager, M., Longo, L., Cole, K.A., Wood, A., Attiyeh, E.F., Laquaglia, M.J., Sennett, R., Lynch, J.E., Perri, P., et al. (2008). Identification of ALK as a major familial neuroblastoma predisposition gene. Nature 455, 930–935.

Okamoto, N., Yamanaka, N., Yagi, Y., Nishida, Y., Kataoka, H., O'Connor, M.B., and Mizoguchi, A. (2009). A fat body-derived IGF-like peptide regulates postfeeding growth in Drosophila. Dev. Cell 17, 885–891.

Oldham, S., Montagne, J., Radimerski, T., Thomas, G., and Hafen, E. (2000). Genetic and biochemical characterization of dTOR, the Drosophila homolog of the target of rapamycin. Genes Dev. 14, 2689–2694.

Perez-Pinera, P., Zhang, W., Chang, Y., Vega, J.A., and Deuel, T.F. (2007). Anaplastic lymphoma kinase is activated through the pleiotrophin/receptor protein-tyrosine phosphatase beta/zeta signaling pathway: an alternative mechanism of receptor tyrosine kinase activation. J. Biol. Chem. 282, 28683–28690.

Polak, P., and Hall, M.N. (2009). mTOR and the control of whole body metabolism. Curr. Opin. Cell Biol. 21, 209–218.

Powers, C., Aigner, A., Stoica, G.E., McDonnell, K., and Wellstein, A. (2002). Pleiotrophin signaling through anaplastic lymphoma kinase is rate-limiting for glioblastoma growth. J. Biol. Chem. 277, 14153–14158.

Puig, O., Marr, M.T., Ruhf, M.L., and Tjian, R. (2003). Control of cell number by Drosophila FOXO: downstream and feedback regulation of the insulin receptor pathway. Genes Dev. 17, 2006–2020.

Randhawa, R., and Cohen, P. (2005). The role of the insulin-like growth factor system in prenatal growth. Mol. Genet. Metab. 86, 84–90.

Rulifson, E.J., Kim, S.K., and Nusse, R. (2002). Ablation of insulin-producing neurons in flies: growth and diabetic phenotypes. Science 296, 1118–1120.

Schubert, M., Brazil, D.P., Burks, D.J., Kushner, J.A., Ye, J., Flint, C.L., Farhang-Fallah, J., Dikkes, P., Warot, X.M., Rio, C., et al. (2003). Insulin receptor substrate-2 deficiency impairs brain growth and promotes tau phosphorylation. J. Neurosci. 23, 7084–7092.

Shi, P., Lai, R., Lin, Q., Iqbal, A.S., Young, L.C., Kwak, L.W., Ford, R.J., and Amin, H.M. (2009). IGF-IR tyrosine kinase interacts with NPM-ALK oncogene to induce survival of T-cell ALK+ anaplastic large-cell lymphoma cells. Blood 114, 360–370.

Shingleton, A.W., Frankino, W.A., Flatt, T., Nijhout, H.F., and Emlen, D.J. (2007). Size and shape: the developmental regulation of static allometry in insects. Bioessays 29, 536–548.

Sjögren, K., Liu, J.L., Blad, K., Skrtic, S., Vidal, O., Wallenius, V., LeRoith, D., Törnell, J., Isaksson, O.G., Jansson, J.O., and Ohlsson, C. (1999). Liver-derived insulin-like growth factor I (IGF-I) is the principal source of IGF-I in blood but is not required for postnatal body growth in mice. Proc. Natl. Acad. Sci. USA 96, 7088–7092.

Slaidina, M., Delanoue, R., Gronke, S., Partridge, L., and Léopold, P. (2009). A Drosophila insulin-like peptide promotes growth during nonfeeding states. Dev. Cell 17, 874–884.

Slupianek, A., Nieborowska-Skorska, M., Hoser, G., Morrione, A., Majewski, M., Xue, L., Morris, S.W., Wasik, M.A., and Skorski, T. (2001). Role of phosphatidylinositol 3-kinase-Akt pathway in nucleophosmin/anaplastic lymphoma kinase-mediated lymphomagenesis. Cancer Res. 61, 2194–2199.

Sousa-Nunes, R., Cheng, L.Y., and Gould, A.P. (2010). Regulating neural proliferation in the Drosophila CNS. Curr. Opin. Neurobiol. 20, 50–57.

Sousa-Nunes, R., Yee, L.L., and Gould, A.P. (2011). Fat cells reactivate quiescent neuroblasts via TOR and glial insulin relays in Drosophila. Nature 471, 508–512.

Stocker, H., Radimerski, T., Schindelholz, B., Wittwer, F., Belawat, P., Daram, P., Breuer, S., Thomas, G., and Hafen, E. (2003). Rheb is an essential regulator of S6K in controlling cell growth in Drosophila. Nat. Cell Biol. 5, 559–565.

Stoica, G.E., Kuo, A., Powers, C., Bowden, E.T., Sale, E.B., Riegel, A.T., and Wellstein, A. (2002). Midkine binds to anaplastic lymphoma kinase (ALK) and acts as a growth factor for different cell types. J. Biol. Chem. 277, 35990–35998.

Taguchi, A., Wartschow, L.M., and White, M.F. (2007). Brain IRS2 signaling coordinates life span and nutrient homeostasis. Science 317, 369–372.

Tapon, N., Ito, N., Dickson, B.J., Treisman, J.E., and Hariharan, I.K. (2001). The Drosophila tuberous sclerosis complex gene homologs restrict cell growth and cell proliferation. Cell 105, 345–355.

Teleman, A.A. (2010). Molecular mechanisms of metabolic regulation by insulin in Drosophila. Biochem. J. 425, 13–26.

Teleman, A.A., Chen, Y.W., and Cohen, S.M. (2005). 4E-BP functions as a metabolic brake used under stress conditions but not during normal growth. Genes Dev. 19, 1844–1848.

Verdu, J., Buratovich, M.A., Wilder, E.L., and Birnbaum, M.J. (1999). Cell-autonomous regulation of cell and organ growth in Drosophila by Akt/PKB. Nat. Cell Biol. 1, 500–506.

Weinkove, D., Neufeld, T.P., Twardzik, T., Waterfield, M.D., and Leevers, S.J. (1999). Regulation of imaginal disc cell size, cell number and organ size by Drosophila class I(A) phosphoinositide 3-kinase and its adaptor. Curr. Biol. 9, 1019–1029.

Weiss, J.B., Suyama, K.L., Lee, H.H., and Scott, M.P. (2001). Jelly belly: a Drosophila LDL receptor repeat-containing signal required for mesoderm migration and differentiation. Cell 107, 387–398.

Wu, M.Y., Cully, M., Andersen, D., and Leevers, S.J. (2007). Insulin delays the progression of Drosophila cells through G2/M by activating the dTOR/dRaptor complex. EMBO J. *26*, 371–379.

Yakar, S., Liu, J.L., Stannard, B., Butler, A., Accili, D., Sauer, B., and LeRoith, D. (1999). Normal growth and development in the absence of hepatic insulin-like growth factor I. Proc. Natl. Acad. Sci. USA *96*, 7324–7329.

Zhang, H., Stallock, J.P., Ng, J.C., Reinhard, C., and Neufeld, T.P. (2000). Regulation of cellular growth by the Drosophila target of rapamycin dTOR. Genes Dev. *14*, 2712–2724.

Zhong, W., and Chia, W. (2008). Neurogenesis and asymmetric cell division. Curr. Opin. Neurobiol. *18*, 4–11.

Zoncu, R., Efeyan, A., and Sabatini, D.M. (2011). mTOR: from growth signal integration to cancer, diabetes and ageing. Nat. Rev. Mol. Cell Biol. *12*, 21–35.

Zou, J., Zhou, L., Du, X.X., Ji, Y., Xu, J., Tian, J., Jiang, W., Zou, Y., Yu, S., Gan, L., et al. (2011). Rheb1 is required for mTORC1 and myelination in postnatal brain development. Dev. Cell *20*, 97–108.